DOUBLE WELL POTENTIAL AS DIFFUSIVE FUNCTION FOR PDE-BASED SCALAR IMAGE RESTORATION METHOD

A. Histace

ETIS UMR CNRS 8051, ENSEA-UCP, 6 avenue du Ponceau, 95014 Cergy, France
aymeric.histace@ensea.fr

M. Ménard

L3i, University of La Rochelle, Pole Sciences et Technologie, 17000 La Rochelle, France
michel.menard@univ-lr.fr

Keywords: Image Diffusion, Double well potential, Directional diffusion, Selectivity.

Abstract: Anisotropic regularization PDE's (Partial Differential Equation) raised a strong interest in the field of image processing. The benefit of PDE-based regularization methods lies in the ability to smooth data in a nonlinear way, allowing the preservation of important image features (contours, corners or other discontinuities). In this article, we propose a PDE-based method restoration approach integrating a double-well potential as diffusive function. It is shown that this particular potential leads to a particular regularization PDE which makes it possible integration of prior knowledge about the gradients intensity level to restore. As a proof a feasibility, results of restoration are presented both on ad hoc and natural images to show potentialities of the proposed method.

1 INTRODUCTION

Since the pioneering work of Perona-Malik (Perona and Malik, 1990), anisotropic regularization PDE's raised a strong interest in the field of image processing. Many regularization schemes have been presented so far in the literature, particularly for the problem of scalar image restoration (see (Histace and Ménard, 2008) for a complete review). In (Deriche and Faugeras, 1996) authors propose a synthetic formulation to express the global scheme of PDE-based restoration approaches. More precisely, if we denote $\psi(\mathbf{r},t): \mathbb{R}^2 \times \mathbb{R}^+ \to \mathbb{R}$ the time intensity function of a corrupted image $\psi_0 = \psi(\mathbf{r},0)$, the corresponding regularization problem of ψ_0 is equivalent to the minimization problem described by the following PDE:

$$\frac{\partial \psi}{\partial t} = c_\xi(\|\nabla\psi\|)\frac{\partial^2 \psi}{\partial \xi^2} + c_\eta(\|\nabla\psi\|)\frac{\partial^2 \psi}{\partial \eta^2} \qquad , \quad (1)$$

where $\eta = \nabla\psi/\|\nabla\psi\|$, $\xi \perp \eta$ and c_ξ and c_η are two weighting functions (also called diffusive functions). This PDE can be interpreted as the superposition of two monodimensional heat equations, respectively oriented in the orthogonal direction of the gradient and in the tangential direction: It is characterized by

an anisotropic diffusive effect in the privileged directions ξ and η allowing a non-linear denoising of scalar image. Eq. (1) is of primary importance, for all classical methods can be expressed in that global scheme: For instance, if we consider the former anisotropic diffusive equation of Perona-Malik's (Perona and Malik, 1990) given by

$$\frac{\partial \psi}{\partial t} = div\left(c(\|\nabla\psi\|)\nabla\psi\right) , \qquad (2)$$

with $\psi(\mathbf{r},0) = \psi_0$ and $c(.)$ a monotonic decreasing function, it is possible to express it in the global scheme of Eq. (1) with

$$\begin{cases} c_\xi = c(\|\nabla\psi\|) \\ c_\eta = c'(\|\nabla\psi\|).|\nabla\psi| + c(\|\nabla\psi\|) \end{cases} \qquad (3)$$

Formulation of Eq. (1) is also interested, for it makes stability study of classical proposed methods possible. What we proposed in this article is a prospective study for the integration of a double well potential as a diffusive function $c(.)$ in Eq. (2). Our aim and motivation for such a study are mainly to show that, firstly, such a choice can lead to a stable PDE-based approach for scalar image denoising that can overpass classical approach of Perona-Malik's from which

it is derived and which presents instability problems as formerly shown in (Catté et al., 1992), and, secondly, that this approach overcomes some drawbacks of the classical methods like corner smoothing or pin-hole effect. Layout of this article is the following one: In section two, we introduce the double well function and derive the corresponding PDE in the global scheme of Eq. (1). We also proposed in that section a study of the stability of the derived PDE compared to the stability of Perona-Malik's approach. Third section is dedicated to experimental and quantitative results. Fourth and last section contains conclusion and discussion.

2 DOUBLE WELL POTENTIAL AND CORRESPONDING PDE

2.1 Diffusive function

The double well potential considered in this article is defined by the following function:

$$c_{DW}(u) = 1 - \phi(u) = 1 - \int_0^u v(\alpha - v)(v - 1)dv . \quad (4)$$

Some graphical representations of Eq. (4) for different values of α are proposed Fig. 1.
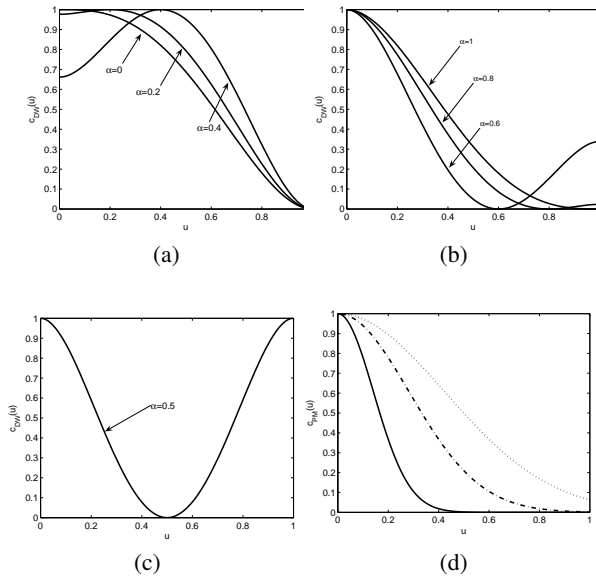
Figure 1: (a), (b), (c) Plots of function $c_{DW}(.)$ of Eq. (4) for different values of α: (a) $0 < \alpha < 0.5$, (b) $0.5 < \alpha < 1$, and (c) $\alpha = 0.5$. (d) Plots of function $c_{PM}(.)$ of Eq. (5) for different values of k and α. Solid lines stand for $k = 0.2$, dash-dotted lines for $k = 0.4$, and dotted lines for $k = 0.6$.

This function has to be compared with the classical Perona-Malik's function $c_{PM}(.)$ given by:

$$c_{PM}(u) = e^{-\frac{u^2}{k^2}} , \quad (5)$$

with k a soft threshold defining selectivity of $c_{PM}(.)$ regarding values of image gradients. Fig. 1.(d) shows graphical representations of $c_{PM}(.)$ defined by Eq. (5) for different values of k. As one can notice on Fig. 1.(d), for $\|\nabla \psi\| \to 0$, $c_{PM}(\|\nabla \psi\|) \to 1$, whereas for $\|\nabla \psi\| \to 1$, $c_{PM}(\|\nabla \psi\|) \to 0$. As a consequence, boundaries within images which are on a threshold, function of k, are preserved from the smoothing effect of Eq. (2). One can notice on Fig. 1 that $\phi(.)$ has been normalized. As a consequence, we are able to ensure that $0 \leq c_{DW}(u) \leq 1$ for all values of u like classical PM's function of Eq. (2). Global variations of c_{DW} can be compared to those of c_{PM} for $\alpha = 0$ and $\alpha = 1$. For $0 \leq \alpha < 1$, since c_{DW} is issued from a double well potential, selectivity of Eq. (2) is more important and centered on a particular gradient value function of α. For instance, for $\alpha = 0.5$, only gradients of value 0.5 are totally preserved from the diffusive effect that can be interpreted as an integration of directional constrains within the restoration process. Moreover, we are now going to show, that integration of c_{DW} as diffusive function leads to interesting stability property of corresponding PDE.

2.2 Study of stability

As mentioned in first section, classical Perona-Malik's PDE presents instability problems. More precisely, as shown in (Catté et al., 1992), sometimes noise can be enhanced instead of being removed. This can be explained considering Eq. (3). If we consider $c_{PM}(.)$ function, it appears that corresponding c_η function of Eq. (3), in the global scheme of Eq. (1), can sometimes takes negative values (see Fig. 2.(a) for illustrations). This leads to local instabilities of the Perona-Malik's PDE which degrades the processed image instead of denoising it. Now, if we calculate mathematical expression of c_η with $c(.) = c_{DW}(.)$ of Eq. (4), one can obtain that:

$$c_\eta(\|\nabla \psi\|) = c'_{DW}(\|\nabla \psi\|).|\nabla \psi| + c_{DW}(\|\nabla \psi\|) , \quad (6)$$

Considering Eq. (6), if we plot this function, one can notice that corresponding c_η function never takes negative values (see Fig. 2.(b) for illustrations): Diffusive process remains stable for all gradient values of processed image which is of primary importance.

3 EXPERIMENTAL RESULTS

We propose in this section to make a visual and quantitative comparison between classical Perona-

(a)

(b)
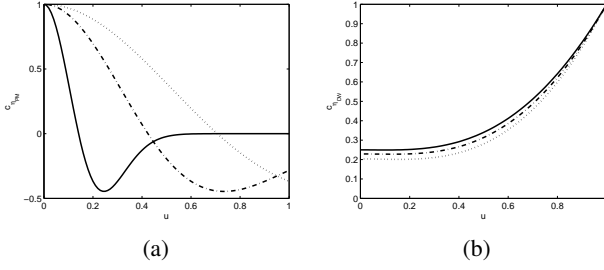
Figure 2: Plots of function $c_{\eta_{PM}}$ and $c_{\eta_{DW}}$ for different values of k and α. Solid lines stand for $k = 0.2$ and $\alpha = 0.5$, dash-dotted lines for $k = 0.4$ and $\alpha = 0.7$ and dotted lines for $k = 0.6$ and $\alpha = 1$.

Malik's PDE of Eq. (2) with diffusive function $c(.) = c_{PM}(.)$ of Eq. (5), and proposed derived PDE with $c(.) = c_{DW}(.)$ of Eq. (4) as diffusive function. For quantitative comparisons, we will consider adapted measure of similarity between non corrupted initial image and restored one. This measure will depend on the nature of original image. For practical numerical implementations, the process of Eq. (2) is sampled with a time step τ. The restored images $\psi(t_n)$ are calculated at discrete instant $t_n = n\tau$ with n the number of iterations.

3.1 Synthetic image

The first proposed image is the binary image of Fig. 3.(a) corrupted by a white gaussian noise of mean zero and standard deviation σ.

(a)

(b)
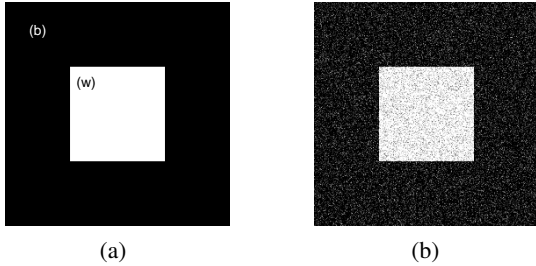
Figure 3: (a) Original synthetic image and (b) its corrupted version ψ_0 . Corrupting noise is a white Gaussian one of mean zero and standard deviation $\sigma = 0.05$.

Considering binary nature of non corrupted image (Fig. 3.(a)), quantification of the denoising effect of Eq. (2) with $c(.) = c_{PM}(.)$ and $c(.) = c_{DW}(.)$, will be estimated with Fisher's index given by

$$I_{Fisher} = \frac{(m_w - m_b)^2}{\sigma_w^2 + \sigma_b^2} \ , \qquad (7)$$

with $m_{w,b}$ the average value of the pixels of the restored image $\psi(t_n)$ being originally in the white (w)

or black (b) part of original image (Fig. 3.(a)) and $\sigma_{w,b}$ the corresponding standard deviation. Because aim of this article is to show potentiality of the described restoration method, only optimal results for both compared approaches are presented Fig. 4: Values of k and α parameters are empirically chosen and strategy for optimal choice is not describe here.

(a)

(b)

(c)
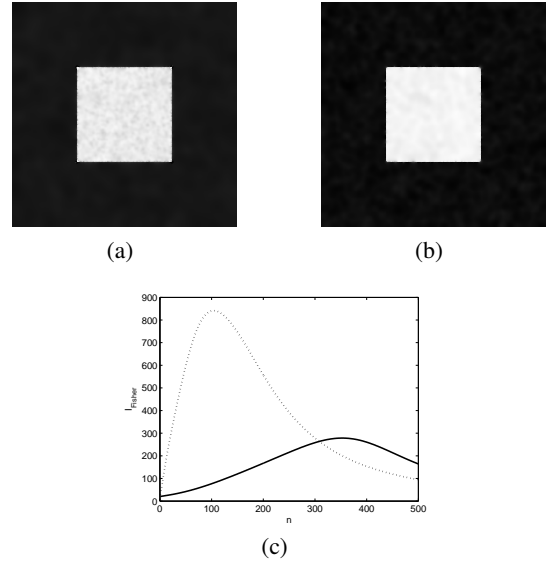
Figure 4: (a) Restored image with $c(.) = c_{PM}(.)$ (classical Perona-Malik's approach), (b) Restored image with $c(.) = c_{DW}(.)$ (proposed approach), (c) Fisher index function of iteration number n, solid lines stands for classical Perona-Malik's approach, dotted line stands for proposed method. k is equal to 0.4, α is equal to 0.5 (these values have been empirically tuned).

As one can notice on Fig. 4, both visually and quantitatively, restoration of binary image of Fig. 3.(a) is better with the diffusive function of Eq. (4). More precisely, stability property of the double well function prevents restoration process from possible enhancement of corrupting Gaussian noise. Homogenous areas of Fig. 4.(b) does not visually shows oscillations, nor corners of the white square as in Fig. 4.(a). This visual impression is confirmed by variations of Fisher's index in Fig. 4.(c) that reaches a level third times more important than with classical approach of Perona-Malik's. The value of α parameter corresponding to best result is 0.5: this is not surprising, for it is also the value of the gradient intensity characterizing the boundaries of the with square. As a consequence, this experiment also confirmed the possible gradient intensity selectivity of the proposed approach interpreted as a directional diffusion process. We shall now experiment the proposed approach in the context of restoration of real scalar images.

3.2 Real images

In this section, we propose to compare both our proposed method with PM's approach on the classical "cameraman" image. For our purpose, this latter has been corrupted by a white gaussian noise of mean zero and standard deviation σ (see Fig. 5).

(a)   (b)

Figure 5: (a) Original image "cameraman" and (b) its corrupted version ψ_0. Corrupting noise is a white Gaussian one of mean zero and standard deviation $\sigma = 0.05$.

Considering nature of non corrupted image (Fig. 5.(a)), quantification of the denoising effect of Eq. (2) with $c(.) = c_{PM}(.)$ and $c(.) = c_{DW}(.)$, will be estimated with a classical PSNR measurement. Once again, because aim of this article is to show potentiality of the described restoration method, only optimal results for both compared approaches are presented Figs. 6 and 7.

(a)   (b)
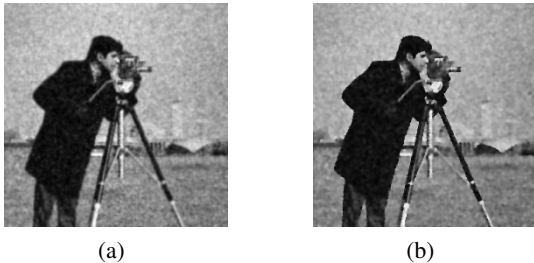
Figure 6: (a) Restored image with $c(.) = c_{PM}(.)$ (classical Perona-Malik's approach), (b) Restored image with $c(.) = c_{DW}(.)$ (proposed approach). k is equal to 1 for PM's restoration approach, α is equal to 0.2 for proposed approach (these values have been empirically tuned).

One can notice on Figs. 6 and 7 that both visually and quantitatively, it is possible to find a value of α that can outperform results of classical PM's approach. Quantitatively speaking PSNR is around 2dB higher and visually speaking, boundaries on Fig. 6 are preserved in a better way from the diffusion effect.

4 CONCLUSION

In this article, we have proposed an alternative diffusive function for restoration of scalar images within the framework of PDE-based restoration approaches.
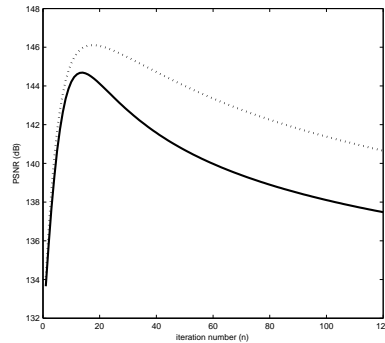
Figure 7: PSNR function of iteration number n, solid lines stands for classical Perona-Malik's approach, dotted line stands for proposed method. k is equal to 1, α is equal to 0.2 (these values have been empirically tuned). These two curves have been computed by calculation of the mean results obtained for one hundred different realizations of the gaussian corrupting noise.

The proposed diffusive function allows integrating prior knowledge on the gradient level to restore thanks parameter α of Eq. (4) and remains always stable on the contrary of classical PM's approach. Proposed method also remains fast and easy to compute. Quantitatively speaking, better restoration results have been obtained. Concerning possible outlooks, this proposed method could be associated to the orientation selectivity of a PDE-based method already presented in the framework of that conference in (Histace et al., 2007). Association of both properties should lead to a restoration method with interesting directional properties for "vision in robotics" area for example.

REFERENCES

Catté, F., Coll, T., Lions, P., and Morel, J. (1992). Image selective smoothing and edge detection by nonlinear diffusion. *SIAM Journal of Applied Mathematics*, 29(1):182–193.

Deriche, R. and Faugeras, O. (1996). Les edp en traitements des images et visions par ordinateur. *Traitement du Signal*, 13(6):551–578.

Histace, A., Courboulay, V., and Ménard, M. (2007). Selective image diffusion for oriented pattern extraction. In *4th International Conference on Informatics in Control, Automation and Robotics (ICINCO)*, pages 270–274.

Histace, A. and Ménard, M. (2008). *Robotics, Automation and Contol Book: PDE based approach for oriented pattern segmentation*, chapter 22, pages 207–218. Intech Education and Publishing.

Perona, P. and Malik, J. (1990). Scale-space and edge detection using anistropic diffusion. *IEEE Transcations on Pattern Analysis and Machine Intelligence*, 12(7):629–639.